

Journal of Materials Chemistry A

Accepted Manuscript



This is an *Accepted Manuscript*, which has been through the Royal Society of Chemistry peer review process and has been accepted for publication.

Accepted Manuscripts are published online shortly after acceptance, before technical editing, formatting and proof reading. Using this free service, authors can make their results available to the community, in citable form, before we publish the edited article. We will replace this *Accepted Manuscript* with the edited and formatted *Advance Article* as soon as it is available.

You can find more information about *Accepted Manuscripts* in the [Information for Authors](#).

Please note that technical editing may introduce minor changes to the text and/or graphics, which may alter content. The journal's standard [Terms & Conditions](#) and the [Ethical guidelines](#) still apply. In no event shall the Royal Society of Chemistry be held responsible for any errors or omissions in this *Accepted Manuscript* or any consequences arising from the use of any information it contains.



Material selection and optimization for highly-stable composite bipolar plates in vanadium redox flow batteries†

Cite this: DOI: 10.1039/x0xx00000x

Minjoon Park, Yang-jae Jung, Jaechan Ryu and Jaephil Cho*

Received 00th January 2012,
Accepted 00th January 2012

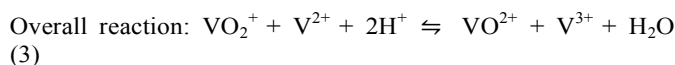
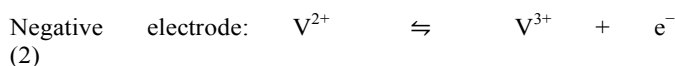
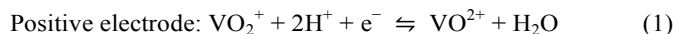
DOI: 10.1039/x0xx00000x

www.rsc.org/MaterialsA

The design of a graphite-based polymer composite bipolar plate is systematically studied for the vanadium redox flow battery system by the compression molding method with different major and minor filler contents. The optimized composite bipolar plate (denoted as the f-GKB-80) composed of flake-type natural graphite (<80 μm) and ketjenblack nanoparticles (<50 nm) exhibits excellent electrical conductivity of 114 S cm⁻¹ and flexural strength of 26 MPa at a total filler loading of 85 wt%. This result can be attributed to the well-developed conducting pathways between the natural graphite flakes that are effectively filled with the ketjenblack minor fillers. Furthermore, this sample is substantially stable even when in storage in highly oxidative V⁵⁺ electrolyte solution at 80 °C for a week. We believe this excellent stability is due to the well-established packing structures, which protect it from concentrated acid-based electrolytes. Significantly, the f-GKB-80 demonstrates enhanced rate capability stable cycling performance including only a 0.87% decay in energy efficiency for 50 cycles compared with commercial graphite plates (2.5% decay in energy efficiency).

Introduction

With the rise in interest in the use of renewable energies such as wind and solar power, the vanadium redox flow batteries (VRFBs) has attracted great attention as a possible grid-scale energy storage system.¹ The VRFBs stack consists of electrodes, membrane separators, current collectors, and bipolar plates.² With the external electrolyte reservoir containing electroactive materials, each of the positive and negative vanadium solutions flows into the battery cells, where charge/discharge reactions occur on the electrode surface through the following reactions:³



The proton exchange membrane controls the proton ion balance between the positive and negative cells with an operation voltage of 1.26 V in the fully charged state. The bipolar plates are one of the main components of flow batteries, preventing direct contact between the electrodes and current collectors.⁴ It is also necessary to have a multi-stack module for the multi-

MWs redox flow system. Out of many research groups, Pacific Northwest National Laboratory (PNNL) has been actively investigated the electrode materials (e.g., bismuth nanoparticles,⁵ niobium nanorod⁶) and stable electrolyte (e.g., mixed acid electrolyte⁷) for high-performance VRFB system.

To date, the research of bipolar plates has been mainly conducted for fuel cell applications.⁸⁻¹¹ The U.S. Department of Energy (DOE) requires the electrical conductivity and flexural strength of bipolar plates to be >100 S cm⁻¹ and >25 MPa, respectively, in fuel cells.⁹ The bipolar plates can be categorized into three types, such as metallic, graphitic, and composite bipolar plates. The metallic bipolar plates have a critical disadvantage in that they are highly corrosive in an acid-based solution, although they do possess good electrical conductivity and formability.¹² The graphitic bipolar plate also has some drawbacks, such as lack of mechanical strength and low processability, resulting in thicker bulky plates, large weight, and high cost.¹³ Thus, the carbon-based polymer composite bipolar plate is considered as a promising alternative to both metal and graphite types, and has attracted much attention in fuel cell system application.¹⁴⁻¹⁶ These composite bipolar plates can be regarded as ideal candidates in terms of electrical conductivity and corrosion resistance.

In contrast to the case of the fuel cell, the composite bipolar plates for the VRFB have not been extensively studied as yet. For instance, the effect of the carbon black contents from 1 to 20 wt% on electrical conductivity and electrochemical stability was reported by Lee et al.¹⁷ They reported that 15 wt% carbon black contents with highest electric conductivity of ca. 30 S cm⁻¹ at led to more stable cycling performance than

School of Energy and Chemical Engineering, Ulsan National Institute of Science and Technology (UNIST), Ulsan, 689-798, South Korea. E-mail: jpcho@unist.ac.kr

† Electronic Supplementary Information (ESI) available: Table S1, and Figure S1–S5. See DOI: 10.1039/b000000x/

conventional pure graphite bipolar plates in VRFB cells. Burak Caglar et al. fabricated the synthetic graphite and carbon nanotube (CNT) filled composite bipolar plates.¹⁸ They used the titanate-based coupling agent to improve the dispersion of fillers, and presented the in-plane and through-plane conductivity of 20 S cm^{-1} and 57.3 S cm^{-1} , respectively. It should be also noted that the bipolar plates for the fuel cell cannot be directly applied in the VRFB due to different operating environments with concentrated acidic vanadium electrolytes.¹⁷ In spite of this emerging factor, no previous studies have reported a systematic study of bipolar plate design processes to achieve mechanically and electrochemically robust flow battery systems.

In this study, the optimal fabrication conditions and filler compositions including the different sizes, shapes, and sources for the VRFB bipolar plates are proposed to realize high electrical conductivity and stability in a concentrated acidic environment. According to this optimization process, the f-GKB-80 composite bipolar plate exceeds the DOE criteria with the an in-plane conductivity of 114 S cm^{-1} and flexural strength of 26 MPa at total filler content of 85 wt% with 15 wt% of epoxy resin.

Experimental

Materials and Bipolar plate fabrication

The commercial aromatic epoxy of diglycidyl ether of bisphenol A (DGEBA, Sigma Aldrich, MW 340 g mol^{-1}) was used as the polymer matrix, and diaminodiphenyl sulfone (DDS, Sigma Aldrich, 97%) with melting temperature of $180 \text{ }^\circ\text{C}$ was used as a curing agent. The supplier and some of the physical properties of the major and minor conductive fillers are listed in Table S1 in detail. First, at a certain ratio of DGEBA and 5% of DDS were dissolved in acetone solution by melt mixing at a temperature of $80 \text{ }^\circ\text{C}$ by balancing stoichiometry of epoxide and amine groups. This solution was poured into the mixture of major and minor filler powders according to various compositions, as shown in Table 1. The composite powders were prepared with stirring for 1 h, followed by drying in an oven at $60 \text{ }^\circ\text{C}$ for 24 h to remove the moisture. These powders were compressed at 40 MPa, and molded at $200 \text{ }^\circ\text{C}$ for 1 h with subsequent cooling to room temperature. Finally, the desired shape of the composite bipolar plates was obtained ($3 \times 4 \text{ cm}^2$ with thickness of 0.3 cm).

Characterization

In-plane conductivity of samples was measured by a conventional four point probe measurement device (CMT-SR2000, AITCO). Test setup for through-plane measurement was designed in our laboratory as shown in Figure S3, and was detailed in a previous research paper.¹⁹ The flexural and compressive strength were measured according to KS M ISO 178, ASTM D 695 respectively via the universal testing machine (WL2100, WITPHLAB). The material morphology was investigated by FE-SEM (S-4800m Hitachi). The acid stability was tested by subjecting a piece of bipolar plate to vanadium electrolyte with oxidation state +5 at $80 \text{ }^\circ\text{C}$ for periods up to 7 days, followed by washing and drying at $60 \text{ }^\circ\text{C}$ for 24 h, then the weight loss of each sample was recorded at an interval of 3 days. The carbon felt (PAN CF-20-3, Nippon carbon) was used respectively as a positive and negative electrode.

Electrochemical test

Cyclic voltammetry was conducted using a typical three electrode cell. The circular bipolar plates were employed as working electrodes with a diameter of 6 mm and were connected by a platinum wire to a reference electrode (Ag/AgCl) and counter electrode (Pt mesh) in 0.1 M VOSO_4 (Sigma-Aldrich, 99.5%) in 3 M H_2SO_4 solution (Sigma-Aldrich, 98%) at a scan rate range of 5 mV s^{-1} . A flow cell was assembled for charge/discharge test. The electrolytes were prepared by dissolving 2 M VOSO_4 in 3 M H_2SO_4 solution. The heat-treated carbon felt electrodes (in air at $500 \text{ }^\circ\text{C}$ for 5 h) with an active area of 5 cm^2 were consecutively used as a positive and negative electrode. Nafion117 ion exchange membrane was employed. The graphite bipolar plate (98.2% graphite, 1.8% ash, Grafoil GTB, GrafTech), without any resin or fillers, was used as a control sample. The graphite bipolar plate and composite bipolar plate were placed between the electrodes and copper current collectors, respectively. The test cell was charged and discharged under an operating potential ranging from 1.65 to 0.8 V with a current density range of 40 mA cm^{-2} to 100 mA cm^{-2} .

Results and discussion

All the carbon-based materials used in this study as either a

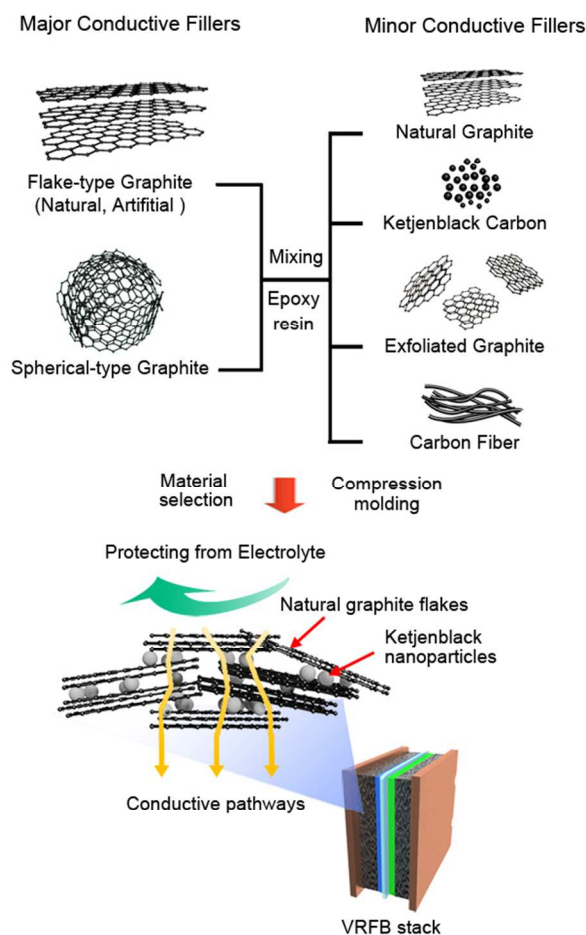


Figure 1. Schematic of the major and minor conductive fillers and the fabrication process of the carbon-based polymer composite bipolar plates for all-vanadium redox flow batteries.

major or minor filler component are presented in Figure 1 and Table S1. The composite bipolar plates were fabricated by using these major filler and minor filler materials with epoxy of diglycidyl ether of bisphenol A (DGEBA) and curing agent of diaminodiphenyl sulfone (DDS) in the five different ratios (Table 1). It was found that the composite bipolar plates with total filler content greater than 90 wt% were fragile and easily fractured. In case of a smaller total filler content of below 60 wt%, it was not possible to fabricate the bipolar plates because of the high viscosity of the composite solutions. Major conductive fillers that serve as the main supports were the flake-type graphite or spherical-type graphite. These major fillers were mixed with a minor conductive filler, such as mill-sized natural graphite, ketjenblack, exfoliated graphite, or carbon fiber. The composite powders were prepared by the solution intercalation method.¹⁹ Specifically, each precursor of the filler was added to the solution of the epoxy resins and curing agent in acetone, followed by stirring for 1 h. After drying the mixtures at 60 °C for 24 h, the dried materials were obtained in powder form. Finally, these powders were molded by hot compression at 200 °C for 1 h (see Experimental section for a detailed description). The dimension of the test samples was 3 × 4 cm² with thickness of 0.3 cm. All of the samples were prepared identically and presented in Figure S1.

Figure 2 presents the SEM images of the prepared composite bipolar plates fabricated with different kinds of major and minor fillers. All of the bipolar plates were fractured to examine the surface morphologies of the cross-sectional planes. First, to investigate the conductive network structure in the composite bipolar plates for the different sizes and morphologies of the major filler, the flake- and spherical-type graphite were used as the major filler components, respectively. The shapes of these two graphite materials have been the most comprehensively investigated for use as conductive fillers in conductive polymer composite applications.^{20, 21} The SEM images of different sized flake-type natural graphite used as major fillers (sized of 5 and 20 μm, denoted as f-GKB-5 and f-GKB-20, respectively) are shown in Figures 2a and b, respectively. Although the ketjenblack particles are homogeneously dispersed on the major filler surface (insets of Figures 2a and 2b), it reveals that the exposed graphite edge planes are gradually amplified as the size of the natural graphite flakes decreases. Figure 2c shows the image of the fracture in the f-GKB-80 bipolar plate consisting of the flake-type natural graphite (sizes of 80 μm) and ketjenblack nanoparticles. The high magnification image of Figure 2c indicates that the ketjenblack are effectively dispersed on the larger graphite flakes. As for the spherical-type of graphite fillers, particles of

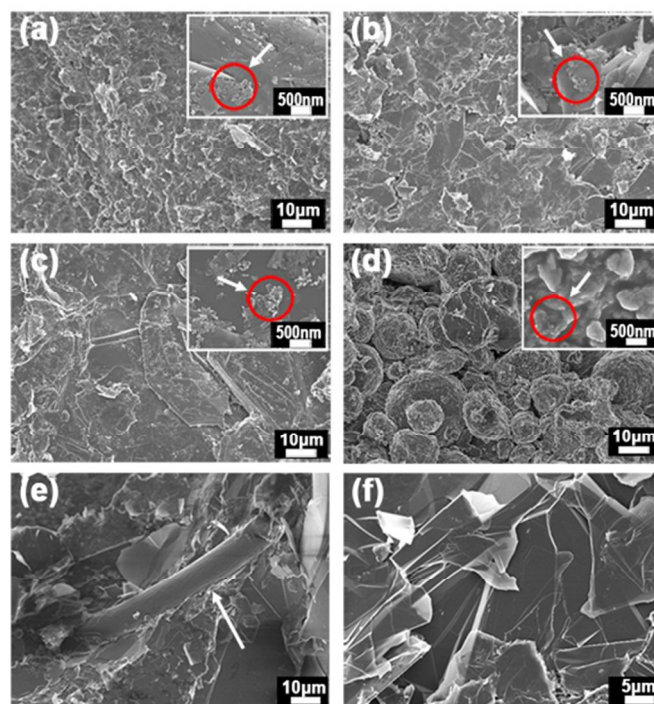


Figure 2. SEM image of the fractured composite bipolar plates with total filler content of 85 wt%. (a–c) Composite bipolar plates with different flake sizes of natural graphite (a: 5 μm, b: 20 μm, and c: 80 μm) and ketjenblack nanoparticles (KB). The insets show the magnified images of a–c, indicating the dispersed KB particles on the natural graphite surface. (d) s-GKB-20 composite of spherical graphite (MCMB, 20 μm) with KB particles, and its magnified image. The red circles indicate the KB agglomerates. (e) f-GCF-80 composite composed of natural graphite (80 μm) and carbon fibers of diameter of ca. 7 μm (white arrow bar). (f) f-GEG-80 composite consisting of natural graphite (80 μm) and exfoliated graphite as minor fillers.

mesocarbon microbeads (MCMB, diameters of 20 μm) and ketjenblack were blended with the epoxy resin (Figure 2d). The voids between the spherical graphite particles were filled by ketjenblack clusters. However, these voids seemed to be relatively larger than those in flake-type natural graphite/ketjenblack composite bipolar plates. In addition to studying a mixture consisting of major fillers of different sizes

Table 1. Composition of major and minor fillers in the composite bipolar plates.

Sample	Major filler (Average particle size)	Minor filler (Average particle size)	Composition of Major filler / Minor filler / Resin (wt%)
f-GKB-5	Natural graphite flake (5 μm)		54 / 6 / 40
f-GKB-20	Natural graphite flake (20 μm)		64 / 6 / 30
f-GKB-80	Natural graphite flake (80 μm)	Ketjenblack carbon (50 nm)	74 / 6 / 20
s-GKB-20	Spherical graphite (20 μm)		79 / 6 / 15
a-GKB-20	Artificial graphite flake (20 μm)		84 / 6 / 10
f-GKB-80		Ketjenblack carbon (50 nm)	78 / 2 / 20
f-GNG-80		Natural graphite flake (5 μm)	76 / 4 / 20
f-GEG-80	Natural graphite flake (80 μm)	Exfoliated graphite (3 μm)	74 / 6 / 20
f-GCF-80		Carbon fiber (7 μm)	72 / 8 / 20
			70 / 10 / 20

and morphologies, the morphology of different graphite sources (e.g., natural graphite and artificial graphite) was investigated (Figure S2). The fractured samples exhibit a similar morphology as the f-GKB-20 samples since the same size (20 μm) and filler shape (flake) was used in the case of the respective major fillers. Next, the cross-sectional morphologies of the composite bipolar plate containing different minor fillers (e.g., a carbon fiber, small natural graphite, or exfoliated graphite) was examined to study the inner structural network. All samples were identically fabricated with natural graphite of flake sizes of 80 μm as a major filler. Figure 2e shows that the carbon fibers were embedded in the natural graphite fillers. Carbon fibers are usually used as thermal and mechanical reinforcements for the composite bipolar plate in fuel cells.²² However, it is believed that the carbon fibers are not an appropriate minor filler component because the large diameter of a fiber (ca. 7 μm) makes them inadequate for filling the voids.²³ The exfoliated graphite was also used as a secondary filler, which originated from the expanded graphite powders (Figure 2f). In the fracture image showing the fracture behavior, it is difficult to distinguish between natural graphite and exfoliated graphite. This can be ascribed to the collapsed structure of the exfoliated graphite fillers when the graphite composites are compressed.

With regard to the formation of electrical conductive networks, the flake-type graphite leads to the creation of smaller voids in the composite bipolar plates in contrast to the spherical-type graphite or carbon fibers.²⁴ Thus, the ketjenblack nanoparticles employed as a minor filler can be homogeneously dispersed and thus fill the voids.²⁵ Such a result can be expected to increase the electrical conductivity by forming proper electrical pathways. Shen et al. investigated the effects of the

major filler size on the electrical conductivity and suggested that a larger filler size can increase the electrical conductivity because of the reduced contact resistance.²⁶ Significantly, it should be noted that the exposed graphite edge planes largely decreased with an increase in the major graphite filler size, in the order of the f-GKB-80 < f-GKB-20 < f-GKB-5 samples as illustrated in Figures 2a–c. Accordingly, it can be expected that the large size of the major filler is capable of protecting the composite bipolar plates from a concentrated acidic electrolyte. Therefore, the f-GKB-80 bipolar plate is expected to improve not only the stability of the vanadium electrolyte but also the electrical properties of the VRFB system.

The electrical conductivity for bipolar plates can be grouped into in-plane and through-plane conductivities, which are important factors for the assembly of multi-stack modules. The in-plane and through-plane conductivities are directly related to the bipolar plate area and the number of stacks, respectively. As shown in Figure 3, these two parameters for the composite bipolar plates with a different loading concentration of each material were measured by the four-point probe and experimental setup designed in our laboratory. Every data point is an average of five individual measurements and the error bar represents the standard deviation of the mean. The electrical in-plane conductivities of major fillers of different sizes, shapes, and sources were obtained by increasing the total filler content from 60 to 90 wt%, where 6 wt% ketjenblack was used as a secondary filler (Figure 3a). All of the composites seemed to obey a classical percolation theory when the total filler concentration was increased, while the conductivity was decreased from its peak value because of the reduced epoxy resin contents to wet fillers.²⁷ At first, the electrical conductivities of major fillers of different sizes (5, 20, and 80 μm) with total filler content from 60 to 90 wt% were examined. It was observed that the in-plane conductivity of the composite bipolar plates increased with an increasing size of the flake-type natural graphite. The highest in-plane conductivity of the f-GKB-80 composite was ca. 110 S cm^{-1} at 85 wt% total filler content, implying that the electrical contact resistance was highly reduced because of the diminishing number of electrical pathways. Secondly, the effects of the filler geometry on the electrical conductivity were investigated by using different shaped graphite fillers such as the flake-type (20 μm , f-GKB-20) and spherical-type (20 μm , s-GKB-20) graphite with respect to filler loading ranging from 60 to 90 wt%. The in-plane conductivities of the f-GKB-20 composite exhibited their highest value of ca. 78 S cm^{-1} with total filler loading at 85 wt%, which was higher than that for the spherical-type graphite based composite bipolar plate. From these results, it can be concluded that effective conductive networks are generated not only by well-stacked major fillers but also by the uniformly dispersed ketjenblack nanoparticles inside the voids. On the other hand, the s-GKB-20 composite plate showed poor processability when the total filler contents were over 80 wt% due to an insufficient amount of epoxy resin to bind the spherical graphite particles with large voids in contrast to the case with the well-packed graphite flakes. Thus, it can be understood that the conductive materials in the composite cannot be kept in such compact conditions as to form sufficient conductive networks without decreasing both processability and electrical conductivity. To investigate the effect of different graphite sources on the electrical conductivity, the artificial graphite (sizes of 20 μm) with ketjenblack nanoparticles, denoted as a-GKB-20 composite was prepared to compare with a composite bipolar plate, the f-GKB-20, fabricated from equal

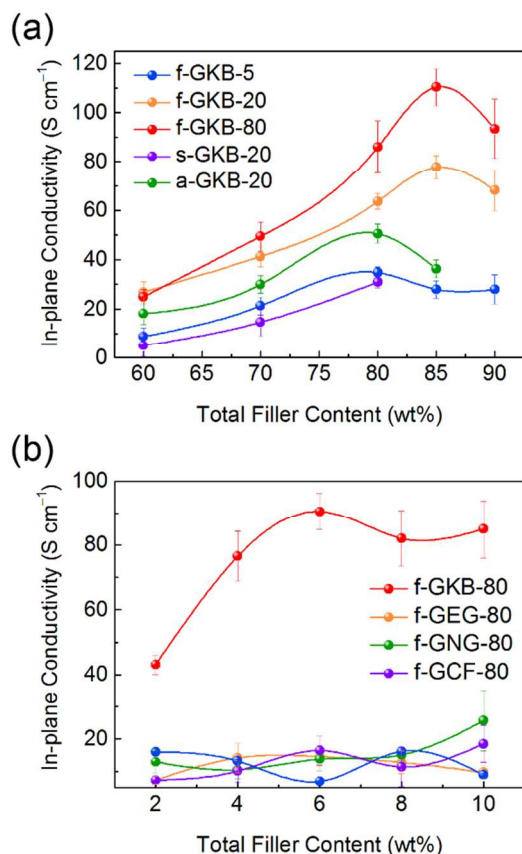


Figure 3. Electrical conductivity of the composites. Effect on (a) major filler types versus total filler contents, in which minor filler contents were fixed to 6 wt%, and (b) minor filler types versus total filler contents. (KB: ketjenblack carbon)

shaped and sized natural graphite. The results clearly show that the in-plane conductivity of the a-GKB-20 is much lower than that of natural graphite-based composite because of the lower crystallinity of the artificial graphite flakes.²¹

The minor fillers with a smaller particle size than the major fillers can effectively fill the voids between the graphite flakes and thus reduce the overall resistance of the composites.¹⁶ Figure 3b shows the electrical conductivity as a function of the type and concentration of five minor fillers of the 80 μm flake-type graphite and 20 wt% epoxy resins. The content of the minor filler samples was increased from 2 to 10 wt%. Surprisingly, only the ketjenblack nanoparticles exhibited an increase of electrical conductivity when the filler content was increased to 6 wt%, while no improvement was observed for other minor fillers such as exfoliated graphite, small natural graphite, or carbon fiber samples. This phenomenon may be ascribed to the size of the minor fillers that can fill the void spaces. As seen in the SEM analysis, the ketjenblack nanoparticles can be distributed on the surface of the flake-type natural graphite fillers and efficiently fill their voids. This filling effect can result in enhanced electrical properties for the nanoparticle-based composite bipolar plates. In addition to in-plane conductivities, the through-plane conductivities for all the samples were measured, and exhibited almost a similar trend as for the in-plane tests, as shown in Figure S4.

The effect of various major and minor filler materials on the electrical conductivity was measured to decide on the optimized filler combination. The f-GKB-80 samples demonstrated well-

developed electric pathway and improved conductivity. Finally, the effective content ratio of the selected materials, i.e., natural graphite flakes with a size of 80 μm and ketjenblack nanoparticles, was investigated as shown in Figure 4. Compared to the f-GKB-80 composite with minor filler content of 6 wt% as displayed in Figure 3a (red line), it was found that 4 wt% of the ketjenblack content was most suitable for the composite bipolar plates, allowing for more improvement of in-plane and through-plane electrical conductivities (Figure 4a). The slopes of both conductivities are sharply increased when the total filler fraction attained ca. 75 wt%, displaying a typical percolation behavior. Notably, the in-plane conductivity with filler loading concentration over 85 wt% exceeded the DOE criteria with the value of ca. 114 S cm^{-1} .

The mechanical properties of the f-GKB-80, an optimal composite bipolar plate, were investigated using the Universal testing machine (UTM). Figure 4b shows the effect of increasing the total filler loading concentration on the flexural and compressive strength. For the flexural strength, the highest value of 29 MPa was obtained at a critical filler loading of 80 wt%. However, a rapidly decreasing flexural strength above a critical filler loading was observed, which may be ascribed to a lack of epoxy resin to bind the composite materials. These results also achieved the DOE criteria of flexural strength (~ 25 MPa) for bipolar plates. The compressive strength has a considerable effect on the stack design due to high compression pressures. Compared to the flexural strength, the compressive strength was not seriously affected when the filler loading was increased, displaying an average value of 26 MPa.

To select the optimal composite bipolar plate for the VRFBs, the electrical and mechanical behavior of various compositions was investigated, and it was found that large-sized natural graphite flake with a small amount of ketjenblack reinforcement (81 wt% of flake-type natural graphite, 4 wt% of ketjenblack, and 15 wt% of epoxy resin) constituted the best combination for a high-performance composite bipolar plate.

The robustness and stability of various composite bipolar

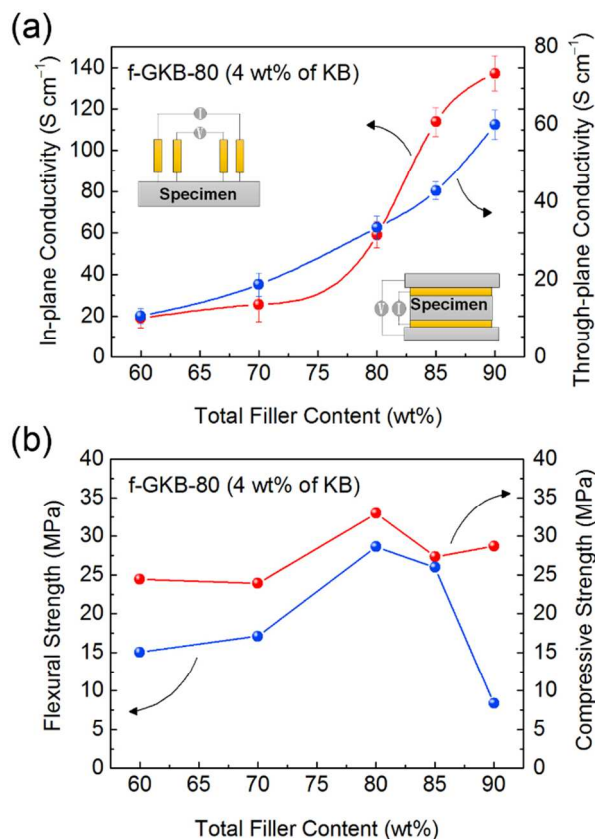


Figure 4. (a) In-plane and through-plane conductivity, and (b) flexural strength and compressive strength versus total filler contents for the f-GKB-80 sample with 4 wt% of KB. (KB: ketjenblack carbon)

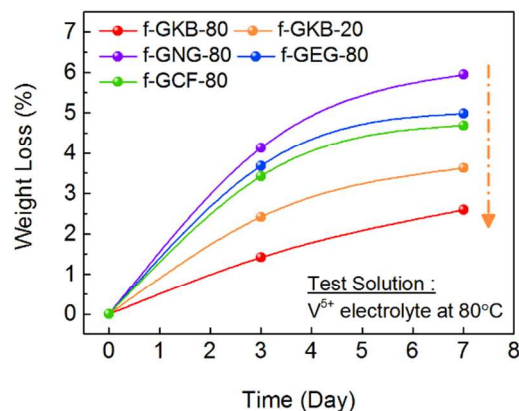


Figure 5. Stability tests of the various types of composite bipolar plates. Weight variation of samples immersed in highly oxidative vanadium electrolyte at 80 °C for 7 days.

plates were tested by using different physical and electrochemical methods. As bipolar plates are continuously used in concentrated acidic conditions, the long-term durability of the prepared samples was investigated by immersing them in highly oxidative V⁵⁺ electrolyte solutions at 80 °C for a week, followed by a weight loss check (Figure 5). Because the V⁵⁺

was a strong oxidant, this electrolyte could impair the materials used in the flow cell.⁷ The data measurement time was fixed at intervals of about three days. After washing each sample and drying it, the weigh variation was examined. The weight loss with different flake sizes of natural graphite (5, 20, and 80 μm) indicated that the durability was proportional to the size of the major fillers, as it indicated that only 2% loss occurred in the f-GKB-80 samples. This result confirms that a large-sized primary filler can effectively protect composite bipolar plates from degradation because of the reduced contact area of the edge sites of the natural graphite flakes. It was evident that the composite bipolar plate with natural graphite flakes of size about 5 μm as major fillers was more or less fractured, so the weight variation could not be checked. This implies that a smaller major filler is vulnerable to a concentrated acidic environment. Next, the effect of different minor filler types was examined. The content of each minor filler was fixed at 6 wt%, and 80 wt% of natural graphite flake (80 μm) was used as a major filler to confirm the stability in vanadium electrolytes. When using the ketjenblack nanoparticles, a remarkable reduction in weight variation was observed. The physical robustness of other composite bipolar plates was found to be poor, and 6% weight loss being exhibited in the f-GNG-80 sample. The high weight degradation of these samples was originated from the large sized minor fillers, which increased not only the voids in the composite plate but also the susceptibility of the plate to the vanadium ions. The commercial graphite plate was also used as a control sample. This sample did not show the weight loss but the increase of weight ca. 2.6% during stability test, which might be contributed to the vanadium reactant on the graphite surface. Consequently, the high stability of the f-GKB-80 bipolar plate can be attributed to physical contact between the natural graphite flakes and the ketjenblack nanoparticles.

Composite bipolar plates must serve as not only a separator between current collectors and electrodes in the stack assembly but also as electrical conducting materials exhibiting chemical inactivity towards vanadium redox species. Thus, the inactivity towards vanadium ions and oxygen evolution, a side reaction, was investigated via the cyclic voltammetry in 0.1 M $\text{VOSO}_4 + 3 \text{ M H}_2\text{SO}_4$ solutions (Figure 6). The test cell was designed for three-electrode system, where the prepared composite bipolar plate, platinum mesh, and Ag/AgCl electrode were used respectively as a working, counter, and reference electrodes. All composite bipolar plates with a diameter of 6 mm were also connected with the Pt wire. For comparison, only Pt wire without bipolar plate samples was tested as a control electrode, exhibiting low activity towards vanadium ions and low oxygen evolution overpotentials due to a small number of active sites and high electron conductivity. In case of carbon-based materials, they apparently display activity towards the vanadium electrolyte, resulting in side reactions. The pronounced oxidation and redox peaks were observed in all composite bipolar plates, compared to the Pt control electrode. Especially, the f-KGB-5 sample shows an extremely increased oxygen evolution current density of 257.3 mA cm^{-2} at 1.6 V vs. Ag/AgCl, which indicates the decomposition of electrolyte solutions. However, the f-GKB-80 sample shows significantly decreased current density of 21.3 mA cm^{-2} at the same voltage. In terms of redox peak currents, these unwanted redox reactions and oxygen evolution side reactions occurred in the order of f-GKB-5 > f-GKB-20 > f-GKB-80. Surprisingly, this order corresponded to the size of major filler, thus implying that the larger size of the natural graphite flakes with small edge sites can be well protected from vanadium electrolytes via highly reduced side reactions.

To demonstrate the practical application of the prepared composite bipolar plate, we used the f-GKB-80 sample as an optimized bipolar plate in the VRFB system (Figure 7a). We assembled the flow-type single cell to evaluate the electrochemical performance and stability. The flow cell was consisting of the composite bipolar plates, Nafion 117 membrane separators, copper current collectors, and heat-treated carbon felt electrodes. The operating voltage was fixed from 0.8 V to 1.65 V to avoid side reactions. For comparison, the commercial graphite plate with graphite content of 98.2% and electrical conductivity of ca. 300 S cm^{-1} was employed as a control bipolar plate. Figure 7a shows the cycle performance and rate capability test of the f-GKB-80 composite and commercial graphite plates for 50 cycles. The charge/discharge current density was increased from 40 to 100 mA cm^{-2} . The coulombic efficiency (CE) of all samples was maintained by

plates have around three times higher electrical conductivity.¹⁴ To

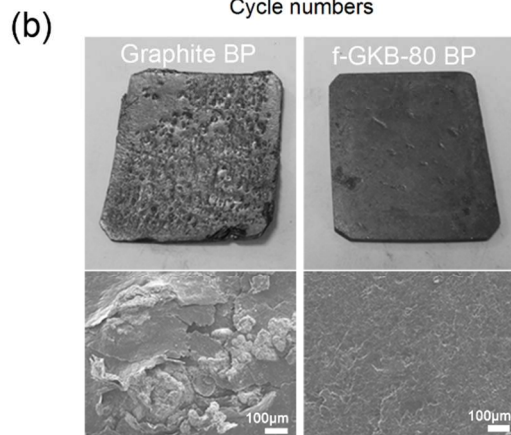
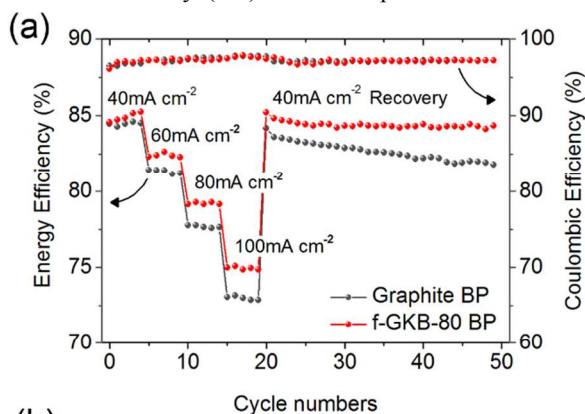


Figure 7. (a) Electrochemical cycling tests of the graphite bipolar plate and f-GKB-80 composite bipolar plate for 50 cycles as functions of energy and coulombic efficiency from 40 to 100 mA cm^{-2} , and (b) digital photographs and SEM images of each sample after the cycling test. (BP: Bipolar plate)

~97% and did not change appreciably during the cycling, which was hardly affected by the bipolar plate samples. The energy efficiency (EE) can be derived from the multiple of the coulombic efficiency and voltage efficiency. At the initial stages with a low current rate of 40 mA cm^{-2} , the EE value of both bipolar plate samples displayed the stable cycling performance, presenting a value of about 85% for 5 cycles. This result implies that there may be critical electrical conductivity for bipolar plates in the VRFB system because they exhibit similar cycling performance, although commercial bipolar

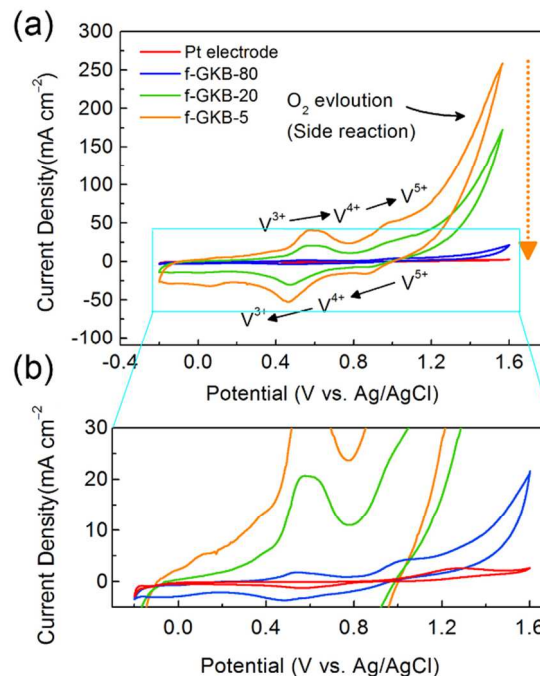


Figure 6. (a) Cyclic voltammograms of the Pt electrode and f-GKB-5, f-GKB-20, and f-GKB-80 samples, (b) showing a high magnification image of (a). (BP: Bipolar plate)

investigate the rate capability, the current density was gradually increased to 100 mA cm^{-2} . Surprisingly, the EE gaps between the two samples were increased as the charge/discharge rate increased. The f-GKB-80 composite bipolar plate achieved an energy efficiency of ca. 75.0% at the rate of 100 mA cm^{-2} , while that of the graphite plates attained the value of ca. 72.8% at the same rate. The origin of the improved rate capability for this composite bipolar plate can be attributed to the significantly reduced overpotentials, as confirmed by the cyclic voltammetry tests. Consequently, to evaluate the robustness of the bipolar plates, the charge/discharge rate was changed from 100 to 40 mA cm^{-2} . When the rate of 40 mA cm^{-2} was recovered, the EE of commercial graphite plates was found to gradually decrease to 81.7% after 100 cycles, a decrease of 2.4% compared to the initial states. Meanwhile, the composite graphite bipolar plate showed excellent cycling stability, demonstrating that only 0.87% of the EE value had been reduced.

In view of the stability, this result was consistent with the physical durability test in Figure 5. Also, it indicates that the f-GKB-80 composite is suitable for bipolar plate applications in the VRFB system, because of the structural robustness towards the concentrated acidic vanadium electrolytes. Significantly, this was also evident from the SEM of both bipolar plates after the cycling test for 100 cycles. Figure 7b shows the surface morphology of the graphite and f-GKB-80 bipolar plates. In case of the graphite bipolar plate, many deep cracks appeared on the surface and detached pieces with a detectable size could be observed by the naked eye. This impaired surface eventually diminished the electrical conductivity, as well as the cycling performance, thus contributing to poor stability. As shown in

the digital photograph of the f-GKB-80 sample, it displayed a clean and smooth surface condition after cycling tests compared with the graphite bipolar plate surface. It is easy to understand that the highly dense structure consisting of the natural graphite flakes and ketjenblack nanoparticles reduces the active sites at the graphite edge planes, thus the f-GKB-80 becomes stable at concentrated acidic conditions.

Conclusions

We investigated the synergistic effect of various major and minor fillers to establish the optimal fabrication conditions for stable composite bipolar plates in the VRFB system. The f-GKB-80 composite bipolar plate with micro-sized major fillers and nano-sized minor fillers exhibited excellent electrical conductivity and mechanical strength. These improved properties are due to the synergistic effect of using larger graphite flakes as the major frame and nano-sized conductive fillers, thus establishing well-developed electron conducting pathways. Such results can be ascribed to the flake geometry with uniformly dispersed ketjenblack nanoparticles in the graphite layer. These nanoparticles are prone to insert themselves into the gaps between the graphite flakes, thus creating the electrical pathways. Furthermore, the f-GKB-80 composite bipolar plate was found to be substantially stable in harsh test conditions due to the well-established packing structures, which protects it from the concentrated acidic electrolytes. In addition to physical properties, the f-GKB-80 demonstrated a stable cycling performance with an energy efficiency decay of only 0.87% after 50 cycles compared with commercial graphite plates (2.5% decay in energy efficiency). We therefore believe that our composite bipolar plates should be suitable for practical industrial applications.

Acknowledgements

This research was supported by MSIP (Ministry of Science, ICT&Future Planning), Korea, under the C-ITRC (Convergence Information Technology Research Center) support program (NIPA-2013-H0301-13-1009) supervised by the NIPA (National IT Industry Promotion Agency). Also, financial support from the BK21 Plus funded by the Ministry of Education, Korea (10Z20130011057) is greatly acknowledged.

References

1. B. Dunn, H. Kamath and J. M. Tarascon, *Science*, 2011, **334**, 928-935.
2. Z. Yang, J. Zhang, M. C. Kintner-Meyer, X. Lu, D. Choi, J. P. Lemmon and J. Liu, *Chem. Rev.*, 2011, **111**, 3577-3613.
3. W. Wang, Q. Luo, B. Li, X. Wei, L. Li and Z. Yang, *Adv. Funct. Mater.*, 2013, **23**, 970-986.
4. P. Qian, H. Zhang, J. Chen, Y. Wen, Q. Luo, Z. Liu, D. You and B. Yi, *J. Power Sources*, 2008, **175**, 613-620.
5. B. Li, M. Gu, Z. Nie, Y. Shao, Q. Luo, X. Wei, X. Li, J. Xiao, C. Wang, V. Sprenkle and W. Wang, *Nano Lett.*, 2013, **13**, 1330-1335.
6. B. Li, M. Gu, Z. Nie, X. Wei, C. Wang, V. Sprenkle and W. Wang, *Nano Lett.*, 2014, **14**, 158-165.
7. W. Wang, Z. Nie, B. Chen, F. Chen, Q. Luo, X. Wei, G.-G. Xia, M. Skyllas-Kazacos, L. Li and Z. Yang, *Adv. Energy Mater.*, 2012, **2**, 487-493.
8. H. Wang and J. A. Turner, *Fuel Cells*, 2010, **10**, 510-519.
9. F. G. Boyaci San and G. Tekin, *Int. J. Energ. Res.*, 2013, **37**, 283-309.

10. V. Mehta and J. S. Cooper, *J. Power Sources*, 2003, **114**, 32-53.
11. A. Hermann, T. Chaudhuri and P. Spagnol, *Int. J. Hydrogen Energ.*, 2005, **30**, 1297-1302.
12. D. Zhang, Z. Wang and K. Huang, *Int. J. Hydrogen Energ.*, 2013, **38**, 11379-11391.
13. R. Taherian, M. J. Hadianfard and A. N. Golikand, *J. Appl. Polym. Sci.*, 2013, **128**, 1497-1509.
14. T. M. Cui, P. Li, Y. Liu, J. X. Feng, M. M. Xu and M. Wang, *Mater. Chem. Phys.*, 2012, **134**, 1160-1166.
15. Y. Q. Sun and G. Q. Shi, *J. Polym. Sci. Pol. Phys.*, 2013, **51**, 231-253.
16. R. A. Antunes, M. C. L. de Oliveira, G. Ett and V. Ett, *J. Power Sources*, 2011, **196**, 2945-2961.
17. N. J. Lee, S. W. Lee, K. J. Kim, J. H. Kim, M. S. Park, G. Jeong, Y. J. Kim and D. Byun, *B. Korean Chem. Soc.*, 2012, **33**, 3589-3592.
18. B. Caglar, P. Fischer, P. Kauranen, M. Karttunen and P. Elsner, *Journal of Power Sources*, 2014, **256**, 88-95.
19. L. Du and S. C. Jana, *J. Power Sources*, 2007, **172**, 734-741.
20. K. C. Li, K. Zhang and G. Wu, *J. Appl. Polym. Sci.*, 2013, **130**, 2296-2302.
21. R. B. Mathur, S. R. Dhakate, D. K. Gupta, T. L. Dhami and R. K. Aggarwal, *J. Mater. Process Tech.*, 2008, **203**, 184-192.
22. J. Simitzis, L. Zoumpoulakis, S. Soulis, D. Triantou and C. Pinaka, *J. Appl. Polym. Sci.*, 2011, **121**, 1890-1900.
23. R. Taherian and M. Nasr, *Int. J. Energ. Res.*, 2014, **38**, 94-105.
24. S. X. Zhou, J. Z. Xu, Q. H. Yang, S. W. Chiang, B. H. Li, H. D. Du, C. J. Xu and F. Y. Kang, *Carbon*, 2013, **57**, 452-459.
25. H. Suherman, J. Sahari and A. B. Sulong, *Ceram. Int.*, 2013, **39**, 7159-7166.
26. L. Shen, H. L. Ding, Q. H. Cao, W. C. Jia, W. Wang and Q. P. Guo, *Carbon*, 2012, **50**, 4284-4290.
27. I. Tavman, I. Krupa, M. Omastova, M. Sarikanat, I. Novak, K. Sever, I. Ozdemir, Y. Seki, S. Podhradská, D. Moskova, E. Erbay and F. Guner, *Polym. Compos.*, 2012, **33**, 1071-1076.

TOC figure

